JVI Journals.ASM.org

CpG Oligodeoxynucleotides Facilitate Delivery of Whole Inactivated H9N2 Influenza Virus via Transepithelial Dendrites of Dendritic Cells in Nasal Mucosa

Tao Qin, Yinyan Yin, Qinghua Yu, Lulu Huang, Xiaoqing Wang, Jian Lin, Qian Yang

Key Laboratory of Animal Physiology and Biochemistry, Ministry of Agriculture, Nanjing Agricultural University, Nanjing, Jiangsu, People's Republic of China

ABSTRACT

The spread of the low-pathogenicity avian H9N2 influenza virus has seriously increased the risk of a new influenza pandemic. Although whole inactivated virus (WIV) vaccine via intranasal pathway is the effective method of blocking virus transmission, the mucosal barrier seems to be a major factor hampering its development. CpG oligodeoxynucleotides, a known adjuvant, can target downstream dendritic cells (DCs) and effectively enhance the mucosal and systemic immune responses. However, the ability of CpGs to assist H9N2 WIV in transepithelial transport remains unknown. Here, *in vitro* and *in vivo*, we showed that CpGs provided assistance for H9N2 WIV in recruiting DCs to the nasal epithelial cells (ECs) and forming transepithelial dendrites (TEDs) to capture luminal viruses. CD103$^+$ DCs participated in this process. Chemokine CCL20 from nasal ECs played a key role in driving DC recruitment and TED formation. Virus-loaded DCs quickly migrated into the draining cervical lymph nodes (CLNs) for antigen presentation. In addition, the competence of CpGs was independent of direct epithelial transport via the transcellular or paracellular pathway. Taken together, our data demonstrated that CpGs enhanced the transport of H9N2 WIV via TEDs of nasal DCs, which might be a novel mechanism for optimal adaptive immune responses.

IMPORTANCE

This paper demonstrates by both an *in vivo* and an *in vitro* coculture model that CpG oligodeoxynucleotides, known as an adjuvant generally targeting downstream immune responses, also are crucial for the transport of H9N2 WIV across nasal epithelial cells (ECs) via the uptake of transepithelial dendrites (TEDs). Our results prove for the first time to our knowledge that the immune-potentiating mechanism of CpGs is based on strengthening the transepithelial uptake of H9N2 WIV in nasal mucosa. These findings provide a fresh perspective for further improvement of intranasal influenza vaccines, which are urgently needed in the face of the potential threat of H9N2 influenza.

The prevention and control of influenza are becoming more and more urgent, especially given the recent avian influenza A (H7N9) outbreaks in China (1). This subtype is primarily reassorted with enzootic H9N2 viruses that have circulated widely among birds in the Far East and the Middle East since the late 1990s (2). Based on their safety profile, high immunogenicity, and the capability of establishing cross-protection at the pathogen's entry site and interrupting viral transmission (3–6), whole inactivated H9N2 influenza vaccines given via intranasal (i.n.) immunization are very effective for virus elimination. Nonetheless, the efficacy of intranasal immunization is currently poor, primarily because of the physiology of the nasal cavity. Antigens have to find their way to overcome a series of barriers (mucus, cilia, and compact epithelium) before they are absorbed into the body (7). Numerous studies have attempted to improve the effect of i.n. whole inactivated virus (WIV) influenza vaccines by using mucoadhesive particulate carrier systems, such as thermal-sensitive hydrogel (8), to prolong the nasal residence time or by using several immunopotentiators, such as interferons and cholera toxin (CT), to target the downstream immune system (9–11).

Our previous study showed that CpG oligodeoxynucleotides, as an i.n. vaccine adjuvant, remarkably enhanced the mucosal and systemic immune responses for inactivated avian influenza viruses, including H5N1, H5N2, and H9N2, when administered to chickens or ducks (3, 12, 13). The investigation of mechanisms by which CpGs enhance the immune response has been mainly focused on the induction of macrophages, dendritic cells (DCs), and B cells through activating the Toll-like receptor 9 (TLR9) or TLR21 and NF-κB signaling pathways, promoting cytokine secretion and the expression of costimulatory molecules, and enhancing the immune response with a tendency toward a Th1-type response (12, 14). However, we do not lose sight of the fact that the nasal mucosa barrier is a key impediment for influenza WIV uptake and subsequent antigen-specific adaptive immune responses, as mentioned above. Therefore, we hypothesize that CpGs play a critical role in the transepithelial delivery of influenza WIV.

Airway DCs, as sentinel cells located beneath the respiratory epithelium, are critical for acquiring and presenting foreign antigens to T cells, a prelude to the initiation of an adaptive immune response (15, 16). One previous study in the gut demonstrated a novel ability in the uptake function of DCs. A seminal study by

Received 4 February 2015 **Accepted** 11 March 2015

Accepted manuscript posted online 25 March 2015

Citation Qin T, Yin Y, Yu Q, Huang L, Wang X, Lin J, Yang Q. 2015. CpG oligodeoxynucleotides facilitate delivery of whole inactivated H9N2 influenza virus via transepithelial dendrites of dendritic cells in nasal mucosa. J Virol 89:5904–5918. doi:10.1128/JVI.00296-15.

Editor: S. Perlman

Address correspondence to Qian Yang, zxbyq@njau.edu.cn.

doi:10.1128/JVI.00296-15

Rescigno et al. has demonstrated that DCs express tight junction (TJ) proteins and penetrate intestinal epithelial monolayers to sample bacteria (17). Further study suggested that lipopolysaccharide (LPS), a major bacterial component, is able to induce DC translocation across the monolayer of gut epithelial cells (18). In human nasal mucosa in allergic rhinitis but not in healthy nasal mucosa, transepithelial dendrites (TEDs) of HLA-DR-positive ($HLA\text{-}DR^+$) and $CD11c^+$ DCs were easily formed (19). Interestingly, DCs may directly capture only those pathogens that actively invade the epithelium (20). These observations raise the possibility that various "foreigners" or "dangers" seem to have the capability of attracting submucosal DCs to capture luminal antigens via TEDs. Unmethylated CpG motifs are present at a much higher frequency in the genomes of prokaryotes than in those of eukaryotes and present danger signals referred to as pathogen-associated molecular patterns (PAMPs) to pattern recognition receptors (PRRs) (21). These findings led us to hypothesize that CpGs could stimulate DCs to capture H9N2 WIV actively across the mucosal barrier. Here, we demonstrate that CpGs assist in the recruitment of nasal mucosal DCs to the nasal epithelium and in their sampling of luminal H9N2 WIV *in vivo*. We confirmed our findings in an *in vitro* DC/epithelial cell (EC) coculture system by using Calu-3 ECs and DCs, which allows simulation of the nasal mucosal barrier in a spatial distribution similar to that found *in vivo*.

MATERIALS AND METHODS

Animals. Wild-type BALB/c and C57BL/6 mice (4 to 6 weeks old) were purchased from the Animal Research Center of Yangzhou University (Yangzhou, China). All efforts were made to minimize the number of animals used and their suffering. The animals were acclimatized for 1 week before the study and had free access to water and standard mouse chow throughout the experiment. The Animal Ethics Committee at Nanjing Agricultural University reviewed the protocol and approved this study specifically, with project number 2009ZX08009-138B.

Reagents and cell lines. Recombinant mouse granulocyte-macrophage colony-stimulating factor (GM-CSF) and interleukin 4 (IL-4) were from PeproTech (Rocky Hill, NJ). RPMI 1640 and modified Eagle's medium alpha (MEM-α) were bought from Invitrogen (Grand Island, NY, USA). Fetal bovine serum (FBS) was from HyClone (Thermo Fisher Scientific, Melbourne, Australia). Hamster anti-CD11c (N418) monoclonal antibody (MAb), rat anti-CD103 (AP-MAB0828) MAb, rat anti-major histocompatibility complex II (MHC-II) (M5/114.15.2) MAb, rabbit anti-CCL20 (macrophage inflammatory protein 3α [MIP-3α]) polyclonal antibody (PAb), and rat anti-SIGN related 1 (SIGN-R1) (ER-TR9) MAb were from Abcam (New Territories, Hong Kong). Rabbit anti-occludin and anti-zonula occludens 1 (ZO-1) PAbs were from Invitrogen. Alexa Fluor 488 or 647 secondary antibodies were from Jackson ImmunoResearch (West Grove, PA). Flow cytometry (fluorescence-activated cell sorting [FACS]) antibodies, including allophycocyanin (APC)- or fluorescein isothiocyanate (FITC)-CD11c, FITC-CD40, FITC-CD80, phycoerythrin (PE)-CD103, peridinin chlorophyll protein (PerCP)-Cy5.5-CD69, PerCP-CD45, APC-CD3, FITC-CD4, or the respective isotype controls, were from eBioscience (San Diego, CA, USA). Cholera toxin (CT) was from Sigma (St. Louis, MO). Chloroquine (CQ) was from Invivogen (San Diego, CA). Alexa Fluor 594-labeled or unlabeled phosphorothioate CpGs (22) with the sequences 5′-GCTAGACGTTAGGT-3′ and 5′-TCAACGTTGA-3′ were synthesized by Invitrogen (Shanghai, China). Calu-3 cells (human bronchial epithelial cell line) are originally derived from the subbronchial epithelium of a lung adenocarcinoma (ATCC, Manassas, VA) and have been used as surrogate nasal epithelium due to their similar biophysical properties, such as forming tight monolayers and, also, secreting mucus when cultured in an air-liquid interface (23, 24).

Preparation of H9N2 WIV. H9N2 influenza virus (A/Duck/NanJing/01/1999) was generously provided by Jiangsu Academy of Agricultural Sciences (Nanjing, China) and purified on a discontinuous sucrose density gradient according to a previously described method (25). Inactivated viruses were prepared at 56°C for 30 min, and samples were inoculated into 10-day-old specific-pathogen-free (SPF) embryonated eggs for three passages to test for complete loss of infectivity. The quantity of viruses was measured by determining the hemagglutinin (HA) protein concentration (the HA concentration was about 35% of the total protein) using a Micro BCA (bicinchoninic acid) protein assay kit (Thermo Fisher Scientific, Waltham, MA, USA) (26). Viruses were labeled with the NHS (*N*-hydroxysuccinimide) ester fluorescent probe DyLight 405, 488, or 633 (Thermo Fisher Scientific) according to the manufacturer's instructions, and unincorporated dye was removed using commercial fluorescent dye removal columns (Thermo Fisher Scientific).

Immunogenicity study. Six-week-old C57BL/6 mice ($n = 12$) were immunized intranasally with H9N2 WIV (5 μg HA) alone or in combination with CpGs (20 μg) or CT (2 μg) three times at 1-week intervals (at 0, 7, and 14 days). The mice were euthanized and samples were collected 28 days after the primary immunization. Nasal, tracheal, and lung lavage fluid samples were obtained by washing the organs with 0.5 ml, 0.2 ml, and 0.5 ml sterile phosphate-buffered saline (PBS), respectively. Hemagglutination inhibition (HI) titers in serum were determined as previously described (27). Specific IgGs (total IgG, IgG1, and IgG2a/c) in serum and secretory IgA in lavage fluid samples were determined by enzyme-linked immunosorbent assay (ELISA) using horseradish peroxidase-conjugated anti-mouse total IgG, IgG1, IgG2a (Santa Cruz Biotechnology, Inc., CA), and IgA (Southern Biotech, Birmingham, AL, USA) as described previously (28). Here, we used an anti-IgG2a isotype which cross-reacts with IgG2c (29), and the titers are reported as IgG2a/c titers. Antibody titers were determined by the endpoint ELISA method as described previously (28). Furthermore, splenic lymphocytes were isolated for analyses of proliferative response using the CCK-8 assay (Beyotime, China) and for analyses of CD69 activation using FACS *in vitro*.

DC/EC coculture system. DCs were generated from femur and tibia bone marrow progenitor cells of 4- to 6-week-old C57BL/6 mice using our advanced method (30). Calu-3 cells were seeded on the upper side of ThinCert membrane inserts (pore size, 3 μm; pore density, 0.6×10^6 cm^{-2}) (Greiner Bio-One, Germany) in a 24-well plate overnight. The medium was only removed from the apical compartment to allow the monolayer to grow at the air interface (31). The cells were maintained for 9 to 13 days until steady-state transepithelial electrical resistance (TEER) of ~300 $\Omega \times cm^2$ was achieved (31). In the coculture system, the filters were turned upside down and then DCs (5×10^5) were cultured on the filter facing the basolateral side of ECs for 4 h to let the cells attach to the filter. The filters were then turned right side up and placed into 24-well plates. The different treatments were incubated, always from the apical side, for the times indicated below. DCs were collected for uptake analyses, phenotype assays, and mixed lymphocyte reaction (MLR) assays. The filters and cells were fixed with 4% paraformaldehyde (PFA) for 30 min at 4°C and processed for confocal microscopy. Basolateral supernatants were collected after 24 h for cytokine assays. In the indirect system, ECs were first incubated with each treatment on the apical surface. At the times indicated below, basolateral supernatants were collected and then tested for stimulation of DCs.

Tissue collection and cryosection. Mice were nasally administered DyLight 488- or 633-labeled H9N2 WIV (5 μg HA) with or without CpGs (20 μg) or the same volume of PBS (0.01 M). Then, the mice were anesthetized and sacrificed at the time after inoculation indicated below. After the removal of irrelevant affiliated tissues, the noses were fixed in 4% PFA overnight and then decalcified for 7 days in decalcifying fluid (10% EDTA, pH 7.4). The noses were frozen in embedding medium (OCT, Torrance, CA) and cut into 8-μm sections for analysis of immunofluorescence as described below. Individual cells were obtained from nasal mucosa-associated lymphoid tissues (NALTs) and cervical lymph nodes (CLNs) by

straining through a 100-μm cell strainer and were stained with FITC-CD11c and analyzed by FACS.

Immunolabeling and confocal microscopy. After being permeabilized in 0.2% Triton X-100 for 5 min and blocked with 5% bovine serum albumin (BSA) for 1 h, the fixed filters were labeled overnight at 4°C with primary antibodies, followed by incubation with fluorescent secondary antibodies for 1 h at room temperature. The primary antibodies were replaced by isotype control antibodies for testing the specificity of the antibodies and the labeling procedure. For the *in vivo* model, cryosections were treated as described above. The filters or cryosections were observed by confocal laser scanning microscopy (CLSM) (LSM 710; Zeiss, Oberkochen, Germany). Cross-section images were collected by Z projection with 0.5-μm increments on the *z* axis and analyzed using Zeiss ZEN 2012 and Adobe Photoshop CS6 (Adobe, San Jose, CA).

Uptake, phenotype, and cytokine assays. *In vitro*, the collected DCs were detected by FACS for fluorescent H9N2 WIV uptake. In addition, after 24 h, DCs were stained with the various fluorescent MAbs or isotype controls and then detected by FACS. The data were analyzed using FlowJo (Tree Star). The levels of IL-12p70 and IL-10 in the collected supernatants were determined by using ELISA kits (eBioscience, San Diego, CA), following the manufacturer's instructions.

MLR assay. To analyze the capacity of DCs to activate T cells, allogeneic T cells were purified from BALB/c mouse lymph nodes by using a $CD4^+$ T cell isolation kit (Miltenyi). Carboxyfluorescein succinimidyl ester (CFSE; Invitrogen)-labeled T cells as responder cells (5×10^5/well) were cocultured in duplicate with DCs (DC/T cell ratios of 1:1 and 1:5) (32). MLR was performed in a 24-well plate for 5 days, and then T cell proliferation was detected by FACS.

Statistical analysis. The results were expressed as the means ± standard deviations (SD) and analyzed with GraphPad Prism 5 software (San Diego, CA). Student's *t* test and one-way analysis of variance (ANOVA) were used to compare results between different groups. Differences were considered statistically significant when the *P* value was <0.05.

RESULTS

CpGs facilitated H9N2 WIV to trigger the local mucosal and systemic immune responses. To verify whether CpGs might function as a nasal mucosal adjuvant for H9N2 WIV, we immunized mice three times intranasally with H9N2 WIV alone or in combination with CpGs or with the known mucosal adjuvant cholera toxin (CT). The locally secreted IgA antibodies, which are the most important characteristics that mediate the nasal adaptive immunity and mucosal protection, were determined. As shown by the results in Fig. 1A, in nasal wash samples, H9N2 WIV plus CpGs or CT was found to have induced much higher IgA specific antibody titers than H9N2 WIV alone. Similar changes in IgA levels in tracheal (Fig. 1B) and lung (Fig. 1C) wash samples were also obtained, suggesting a remarkable effect of CpGs on mucosal responses in the lower respiratory tract. Specific serum IgGs and their subtypes were also detected by ELISA. As shown by the results in Fig. 1D, E, and F, respectively, the levels of IgG, IgG1, and IgG2a/c induced by H9N2 WIV plus CpGs or CT were significantly higher than the levels induced by H9N2 WIV alone. The HI titer profile exhibited a similar change. Serum collected from mice immunized with H9N2 WIV plus CpGs or CT showed a great capability to inhibit hemagglutination against 4 HI units/25 μl of reference antigens (Fig. 1G). Splenocytes isolated from the immunized mice and restimulated with H9N2 WIV *in vitro* were assessed for the expression of CD69, an activation marker. We found that splenocytes from the group that received H9N2 WIV plus CpGs or CT were more activated than those from the group that received H9N2 WIV alone (Fig. 1H and I). Moreover, their proliferative index was markedly increased (Fig. 1J). FACS analysis of T cell subtypes from the isolated splenocytes showed that the percentage of $CD3^+$ $CD4^+$ T cells was significantly increased after immunization with H9N2 WIV plus CpGs ($P < 0.01$) or CT ($P < 0.01$) compared with the percentage after immunization with H9N2 WIV alone (Fig. 1K). Altogether, these results demonstrated that intranasal vaccination with H9N2 WIV plus CpGs effectively induced local mucosal and systemic immune responses.

CpGs facilitated H9N2 WIV to enhance DC maturation both in the monoculture and coculture system. DC maturation is a key step for the subsequent antigen-specific immune response (33). However, it is still unclear how DC maturation works in nasal mucosal immunity. Thus, we assessed DC maturation in the presence of an epithelial barrier (coculture system, containing Calu-3 ECs and DCs *in vitro*) (Fig. 2Ab) or without an epithelial barrier (monoculture, direct contact between DCs and H9N2 WIV/CpGs) (Fig. 2Aa). Phenotype maturation of submucosal DCs was detected after 24 h. In monoculture, H9N2 WIV and/or CpGs strongly upregulated the expression of CD40 and CD80 compared with the results for medium. In the coculture system, although the levels of stimulation of CD40 and CD80 by H9N2 WIV were lower than the levels in monoculture, CpGs had a powerful ability to increase their expression (Fig. 2B to D). Furthermore, the release of cytokines (IL-12p70 and IL-10) represents functional maturation of DCs. Similarly, H9N2 WIV plus CpGs significantly increased their secretion in both models compared with the results for H9N2 WIV alone (Fig. 2E and F, respectively). Finally, to test fully functional maturation of DCs, DCs were assessed for their ability to stimulate allogeneic T cells. As expected, the DCs from the group treated with H9N2 WIV plus CpGs strongly enhanced the proliferation of allogeneic T cells compared to the results for the H9N2 WIV-only group (Fig. 2G). Of note, in the above-described experiments, pretreatment of ECs with chloroquine (CQ; a TLR9 inhibitor that blocks the interaction between TLR9 and CpGs via endosomal acidification [34]) reversed the effect of CpGs, suggesting that CpGs first participated in EC activation. Taken together, these results implied that CpGs still facilitated H9N2 WIV to enhance DC maturation in the presence of an epithelial barrier.

CpGs increased the number of H9N2 WIV-loaded submucosal DCs in the DC/EC coculture system. Direct contact between submucosal DCs and luminal antigens is required for triggering DC maturation and subsequent adaptive immune responses. Thus, we tested whether CpGs could increase the number of H9N2 WIV-loaded submucosal DCs in the DC/EC coculture system. In the coculture system, the number of virus-loaded submucosal DCs was greatly increased at an early stage (20 min to 1 h) as determined by using CLSM (Fig. 3B and C) and FACS (Fig. 3D and E). These findings suggested that CpGs were involved in increasing viral uptake by submucosal DCs.

ECs were not essential for the transepithelial transport of H9N2 WIV with the presence of CpGs. To confirm whether CpGs could disturb the epithelial barrier to allow viral delivery, we first determined their effect on the cell viability of ECs and DCs. We found that CpGs did not decrease the cell viabilities of ECs and DCs (data not shown). Given that CpGs provide assistance for transepithelial transport of H9N2 WIV via the paracellular route of ECs, the transepithelial electric resistance (TEER) and tight junction proteins were determined in the coculture system (Fig. 4A). CpGs did not change the TEER, whereas CT (both 100 ng/ml

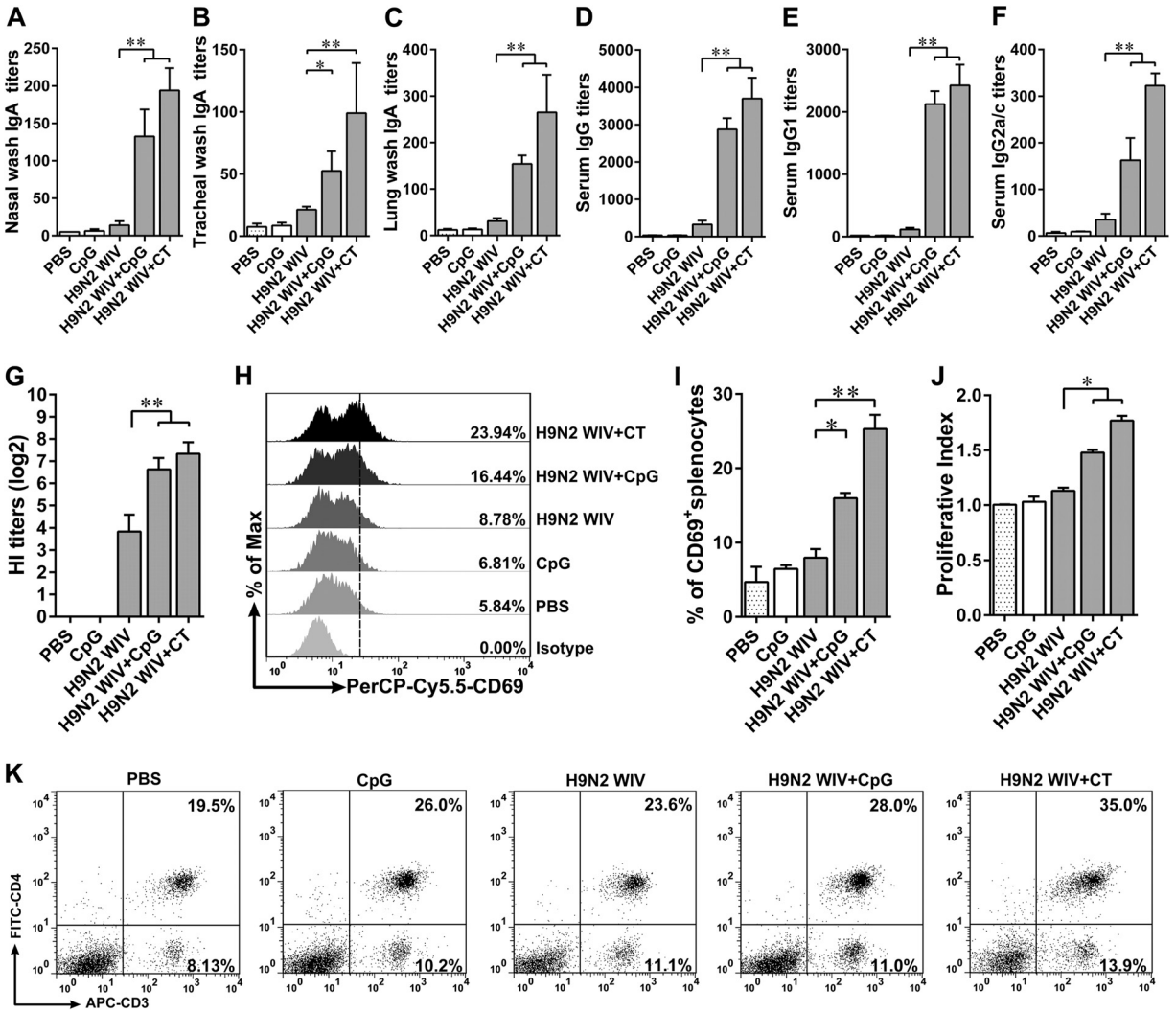

FIG 1 H9N2 WIV-specific local mucosal and systemic immunity after intranasal immunization of mice. (A to C) At 28 days after the primary immunization, H9N2 WIV-specific mucosal IgA titers in nasal wash (A), tracheal wash (B), and lung wash (C) were determined by endpoint ELISA. (D to F) H9N2 WIV-specific IgG (D), IgG1 (E), and IgG2a/c (F) titers in serum were determined by endpoint ELISA. (G) Serum hemagglutination inhibition (HI) levels after immunization. Antibody titer was detected by HI assay using 4 hemagglutinating units of the influenza virus strain. (H to J) Splenocytes were restimulated by H9N2 WIV (10 μg/ml) following 72 h *in vitro*. (H and I) FACS analysis of splenocyte activation (assessed as CD69 expression). (J) CCK-8 assay was used to analyze splenocyte proliferation. (K) FACS analysis of T cell subtypes of splenocytes isolated from the immunized mice. The data shown are the mean results ± SD. *, $P < 0.05$; **, $P < 0.01$.

and 1 μg/ml) decreased the TEER as early as 0.5 h (Fig. 4B), suggesting that CT impaired the barrier function of ECs. Similarly, there were no significant changes in the localization of the tight junction proteins occludin (Fig. 4D) and ZO-1 (Fig. 4G) with CpG treatment compared to their localization with medium alone (Fig. 4C and F, respectively). However, in CT-treated cells, occludin expression followed an abnormal discontinuous distribution (Fig. 4E, arrowheads), and ZO-1 expression appeared to be partially lost (Fig. 4H, arrowheads), suggesting that CT impaired the barrier function of ECs for antigen delivery. Furthermore, given that ECs might participate in transepithelial transport of H9N2 WIV in the presence of CpGs, an indirect system was established (Fig. 4I). FACS analyses of the collected DCs showed that the fluorescence-labeled H9N2 WIV did not appear in DCs until 1 h (Fig. 4J and K). Analysis of the transmission electron microscope (TEM) images showed that H9N2 WIV only attached to the apical surface of ECs and did not enter into the ECs after CpG treatment (Fig. 4L and M), implying that the transport of H9N2 WIV was independent of epithelial direct participation. However, for the specialized epithelial cells, such as M cells, further research is needed.

CpGs facilitated H9N2 WIV recruitment of submucosal DCs to form TEDs *in vitro* and *in vivo*. To investigate whether CpGs have the capability of recruiting submucosal DCs to form TEDs for viral capture, we assessed TED formation *in vitro* and *in vivo*. In the *in vitro* DC/EC coculture system, H9N2 WIV and/or CpGs but not medium, when seeded on the apical side of Calu-3 cells, induced submucosal DCs to form TEDs across ECs all the way to the apical side, as shown in cross-sectional images (Fig. 5B to E). Compared to the results for H9N2 WIV alone, the number of TEDs in the group treated with H9N2 WIV plus CpGs was greatly increased at an early stage (20 min to 1 h) (Fig. 5F). *In vivo*, after

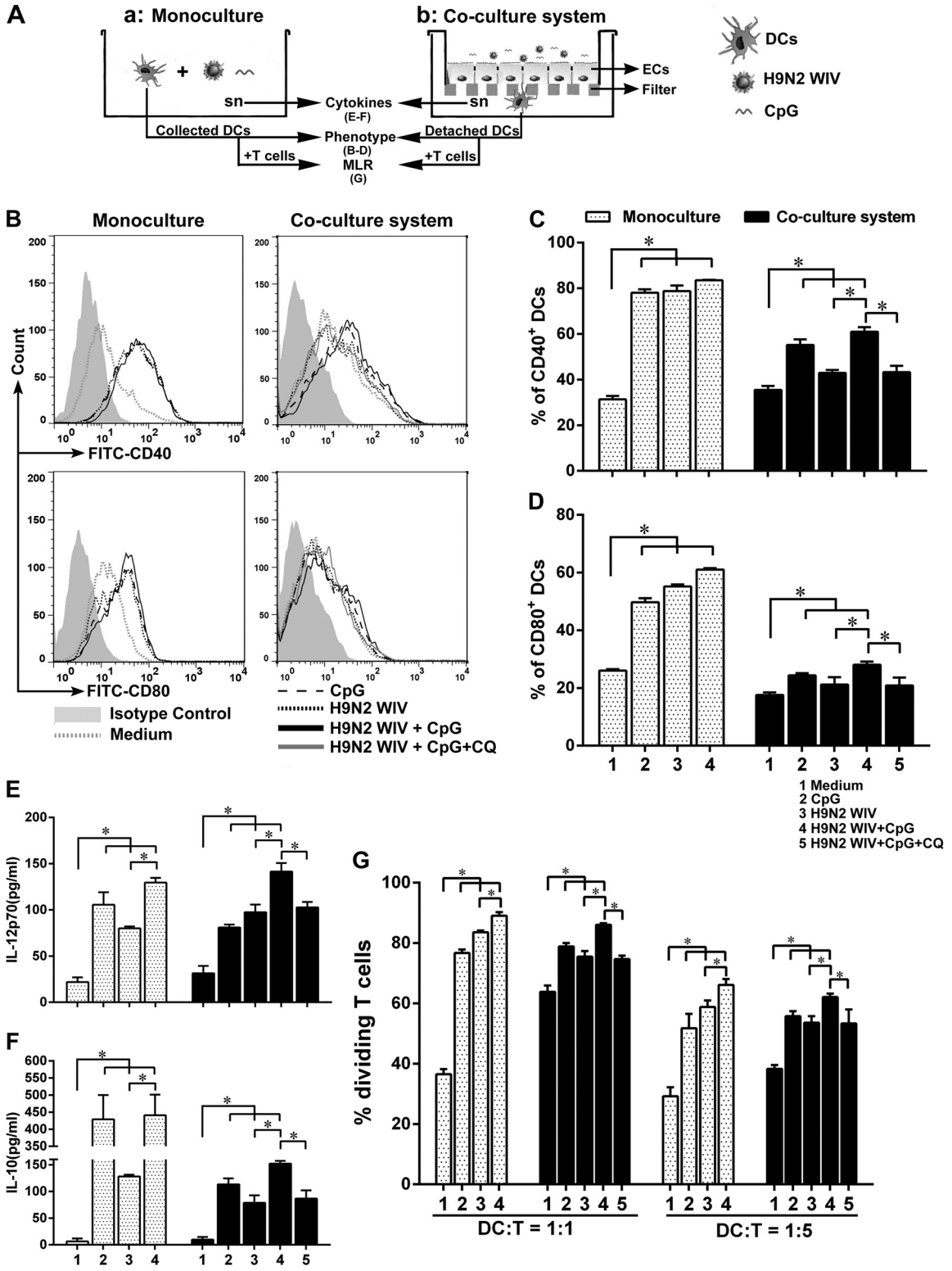

FIG 2 DC maturation both in the monoculture and DC/EC coculture system after CpG challenge. (A) Experimental setting to study DC maturation in two culture systems. Schematic depicts the monoculture system, where H9N2 WIV alone or plus CpGs interacted directly with DCs (a), and the DC/EC coculture system, where ECs were preincubated with CQ (10 μM) or not for 0.5 h before being cocultured with DCs and H9N2 WIV alone or plus CpGs was incubated on the apical side of the ECs (b). After 24 h, DCs and basolateral supernatants were collected for detecting phenotype, cytokines, and MLR. (B to D) The levels of expression of CD40 and CD80 were analyzed by FACS. (E and F) Levels of IL-12p70 (E) and IL-10 (F) release in culture supernatants were measured by ELISA. (G) In MLR experiments, the collected DCs were used in two graded cell numbers (DC/T cell ratios of 1:1 and 1:5) to stimulate CFSE-labeled naive $CD4^+$ allogeneic T cells. After 5 days, proliferation was detected by FACS. (C to G) Treatments are indicated by the shading and numbering of the bars as shown in the keys. The data shown are the mean results ± SD from three independent experiments. *, $P < 0.05$.

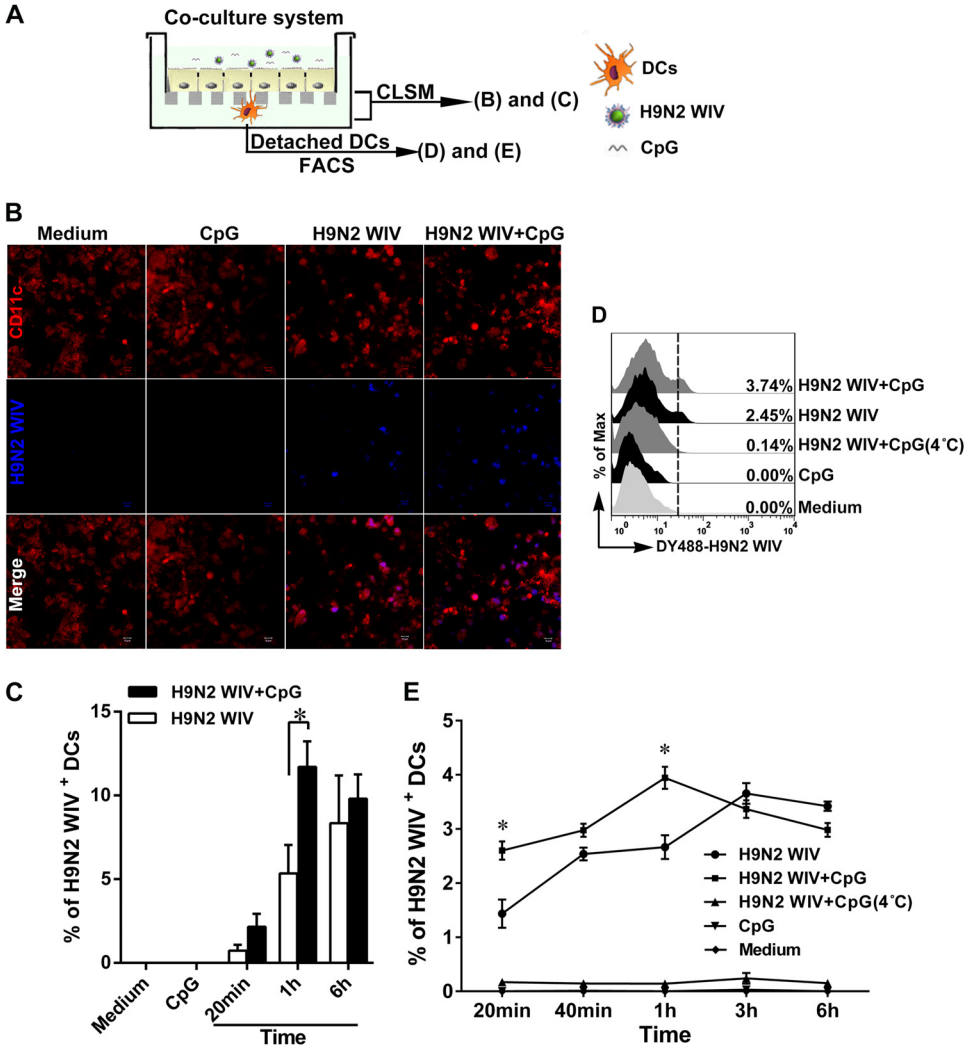

FIG 3 Enhancement of H9N2 WIV uptake by submucosal DCs after CpG addition in the DC/EC coculture system. (A) Schematic of experimental setting to study the viral uptake in the coculture system. DCs were seeded on the underside of the filter facing the basolateral membrane of ECs for 4 h, and then, medium, H9N2 WIV (50 μg/ml HA), and/or CpGs (10 μg/ml) were incubated on the apical side of ECs. (B) Uptake of H9N2 WIV by submucosal DCs was determined using immunofluorescence. After 1 h, the filters in the coculture system were processed and views from between the DCs and the filter were obtained by CLSM. CD11c DCs (red) attached to the underside of the filter. DyLight 405-labeled H9N2 WIV (blue) existed within the submucosal DCs. Bars, 10 μm. (C) Quantification of virus-loaded submucosal DCs from fluorescence images. Values were calculated from six random fields of view (0.044 mm^2 per field) for each of three individual filters. (D and E) FACS analysis of virus-loaded submucosal DCs. DCs were collected from the coculture system after 1 h (D) or after the indicated times (E) and detected by FACS. The data shown are the mean results ± SD from three independent experiments. *, $P < 0.05$.

intranasal administration of H9N2 WIV plus CpGs to mice for 0.5 h, TEDs were apparent in the single-layer (Fig. 5K) or pseudostratified (Fig. 5I, J, L, and M) epithelium. The number of TEDs induced by H9N2 WIV plus CpGs was significantly increased compared to the number induced by H9N2 WIV alone at an early stage (0.5 h) ($P < 0.01$) (Fig. 5N). However, we did not detect any TEDs in the NALT until 2 h (data not shown). Next, we confirmed that another DC surface marker, MHC-II, was also expressed in TEDs (Fig. 5O). Furthermore, $CD103^+$ subset DCs were found to participate in TED formation in the nasal passage, as determined by using CLSM and FACS (Fig. 5P to T). Taken together, the data from the *in vitro* and *in vivo* studies suggested that CpGs have the ability to induce submucosal DCs to generate TEDs in the nasal passage.

Luminal H9N2 WIV were sampled by TEDs *in vitro* and *in vivo*. To determine whether H9N2 WIV could be sampled by TEDs, fluorescence-labeled H9N2 WIV plus CpGs were seeded on the apical side of ECs in the coculture system. We used CMTMR (5-[and-6]-{[(4-chloromethyl)benzoyl]amino}tetramethylrhodamine) cell-tracking dye (CellTracker Orange CMTMR; Molecular Probes, Eugene, OR), following the manufacturer's instructions, and in *z*-orthogonal views from CLSM, CMTMR-labeled DCs were clearly visualized sending TEDs across the TJs of ECs and internalizing luminal H9N2 WIV (Fig. 6A to D, arrow). Some of the viral particles presented bulk and shapes that suggested they may have been aggregated by TEDs. Only sporadic viruses were found at the epithelial surface. Analogously, *in vivo*, the capture of luminal H9N2 WIV by TEDs was

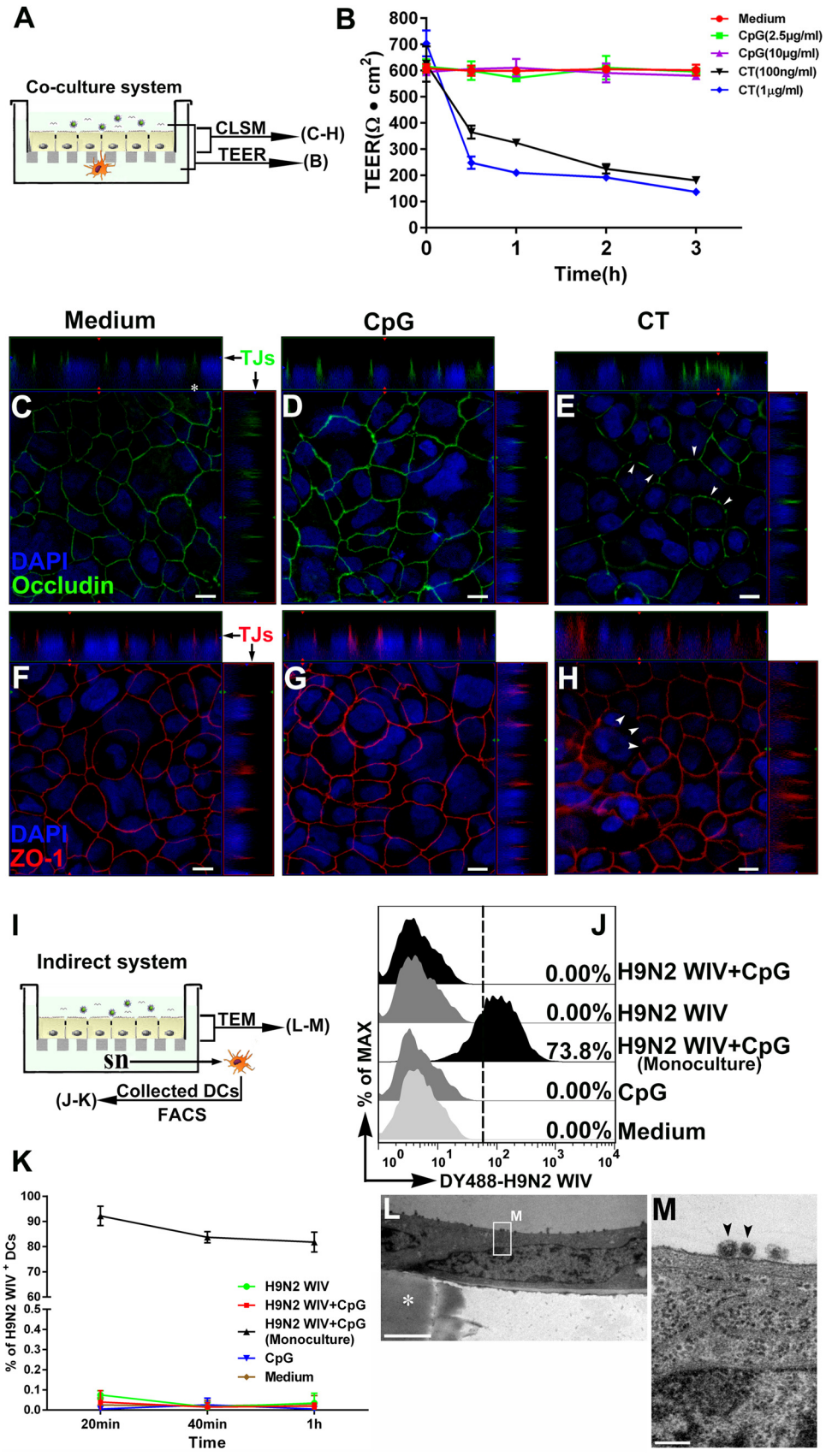
A
Co-culture system
CLSM
(C-H)
TEER
(B)
B
TEER(Ω • cm²)
Time(h)
Medium
CpG(2.5μg/ml)
CpG(10μg/ml)
CT(100ng/ml)
CT(1μg/ml)
Medium
CpG
CT
TJs
C
D
E
DAPI
Occludin
TJs
F
G
H
DAPI
ZO-1
I
Indirect system
TEM
(L-M)
sn
(J-K)
Collected DCs
FACS
J
0.00% H9N2 WIV+CpG
0.00% H9N2 WIV
73.8% H9N2 WIV+CpG
(Monoculture)
0.00% CpG
0.00% Medium
% of MAX
DY488-H9N2 WIV
K
% of H9N2 WIV⁺ DCs
H9N2 WIV
H9N2 WIV+CpG
H9N2 WIV+CpG
(Monoculture)
CpG
Medium
20min
40min
1h
Time
L
M
M

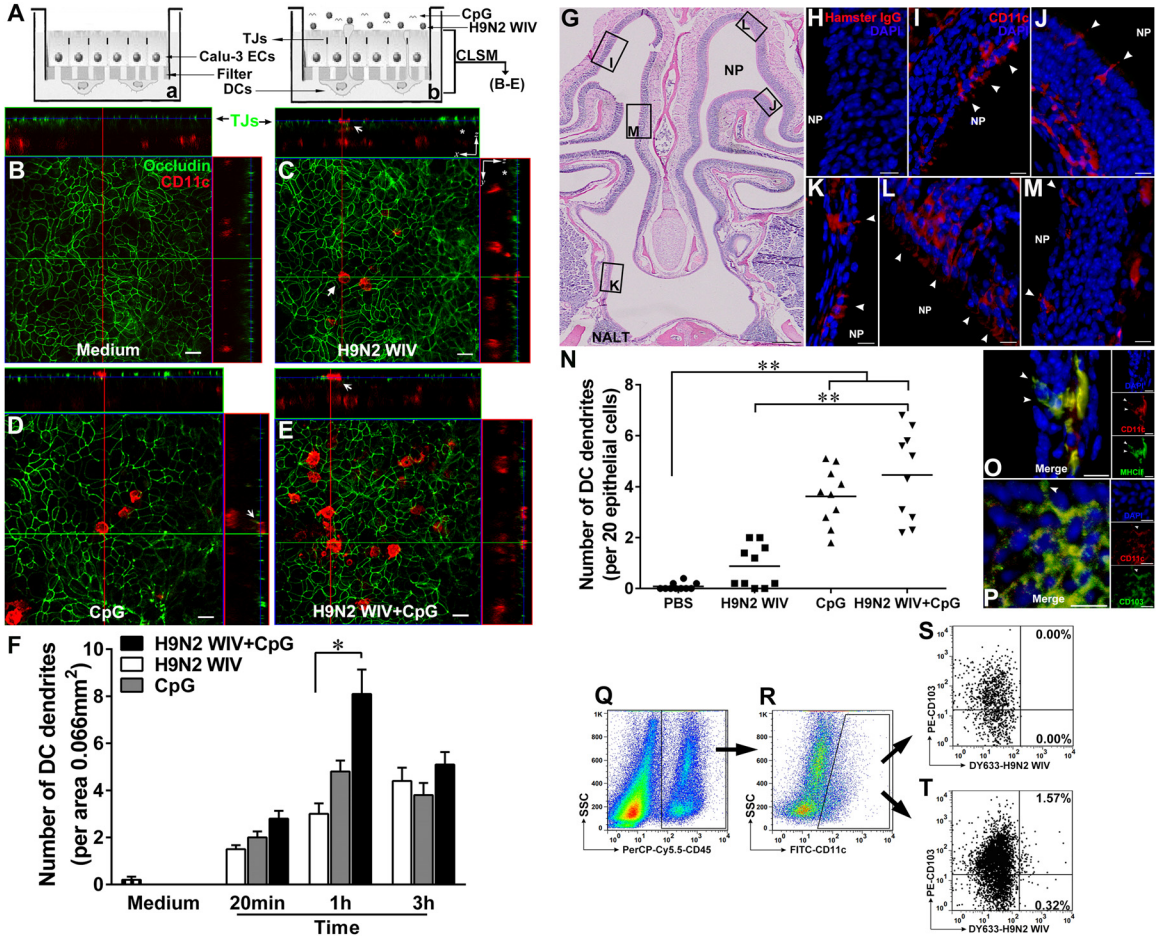

FIG 5 CpGs assist H9N2 WIV in TED formation *in vitro* and *in vivo*. (A) In the DC/EC coculture system, medium (a) or H9N2 WIV and/or CpGs (b) were incubated on the apical side of the ECs for 1 h. Filters were processed for CLSM. (B to E) Cross-sectional images were obtained using ZEN 2012 software. Submucosal DCs (CD11c, red) sent dendrites (white arrow) to creep through the tight junctions (TJ) of ECs (occludin, green) in response to H9N2 WIV and/or CpGs but not medium. (F) Quantification of the numbers of TEDs at the indicated times. Values are expressed as the mean results ± SD from six random fields (0.066 mm^2 per field) for each of three individual filters. The results shown are from a representative experiment out of three. (G to P) Mice ($n = 10$ per group) were nasally administered PBS, H9N2 WIV, and/or CpGs for 0.5 h, and noses were collected. (G) Cross-section of the murine nasal cavity using hematoxylin and eosin (H&E) staining. NP, nasal passage; NALT, nasal-associated lymphoid tissue. Enlarged CLSM images of the regions in the black frames are shown in panels I to M. (H) Isotype control. (I to M) DCs (CD11c, red), nuclei (DAPI, blue), and TEDs (arrowheads). (N) The number of TEDs was quantified. Values are expressed as the number of TEDs per 20 ECs. Each dot represents the value obtained from one nose. Horizontal lines across the scatter plot represent mean values. (O and P) CLSM analyses of surface marker MHC-II and $CD103^+$ DCs involved in TED formation after CpG challenge. CD11c, red; DAPI, blue; MHC-II (O) and CD103 (P), green; TEDs, arrowheads. (Q to T) For FACS analyses, NALTs were removed from noses, and the individual cells isolated from the nasal passages were gated based on $CD45^+$ (Q) for hematopoietic cells. The gated cells were further selected based on $CD11c^+$ (R). SSC, side scatter. (S and T) FACS detection of viral uptake by $CD103^+$ DCs in mice that received PBS (S) or DyLight 633-labeled H9N2 WIV and CpGs (T). *, $P < 0.05$; **, $P < 0.01$. Bars: 20 μm (B to E); 250 μm (G); 10 μm (H to M); 10 μm (O and P).

successfully detected in the nasal passage (Fig. 6E). In the zones enlarged in Fig. 6F to M, the TEDs which colocalized with the viruses (Fig. 6F to I, arrow) and the virus-loaded DCs that moved away from the ECs (Fig. 6J to M, arrowheads) were clearly visible. In addition, $CD103^+$ DCs were participants in the uptake of H9N2 WIV (Fig. 5Q to T). However, CpGs did not have any effect on viral uptake in nasal-associated lymphoid tissue (NALT) at an early stage (0.5 h) (data not shown).

FIG 4 Role of ECs in transepithelial transport of H9N2 WIV after CpG challenge. (A) Schematic of the coculture system. (B) Detection of transepithelial electric resistance (TEER), monitored with a Millicell ERS-2 V-Ohm meter (Millipore, USA), at the indicated times after apical incubation with CpGs (2.5 μg/ml or 10 μg/ml) or CT (100 ng/ml or 1 μg/ml). Data are presented as mean results ± SD from six replicates. (C to H) In views taken between the apical side of ECs and the filter, cross-sectional CLSM images show the localization of the tight junction proteins occludin and ZO-1 (C to E and F to H, respectively) after incubation of medium (C and F), CpGs (10 μg/ml) (D and G), or CT (100 ng/ml) (E and H) on the apical side of ECs for 2 h. (I) Schematic of the indirect system. H9N2 WIV and/or CpGs were seeded on the apical side of ECs for 20 min, 40 min, and 1 h, and then the supernatants (sn) from the basolateral side were collected and incubated with DCs for 20 min, 40 min, and 1 h. (J and K) FACS analysis of virus-loaded DCs. Viral uptake after CpG treatment in monoculture was determined as a positive control. DCs were collected from the indirect system at 1 h (J) or at the indicated times (K) and detected by FACS. (L and M) After 1 h, the filters were processed for TEM. An enlargement of the region in the white frame in panel L is show in panel M. H9N2 WIV were only discovered on the apical surface of ECs (arrowheads). The asterisk indicates the filter. The results shown are from a representative experiment out of three. Bars: 10 μm (C to H); 2 μm (L); 200 nm (M).

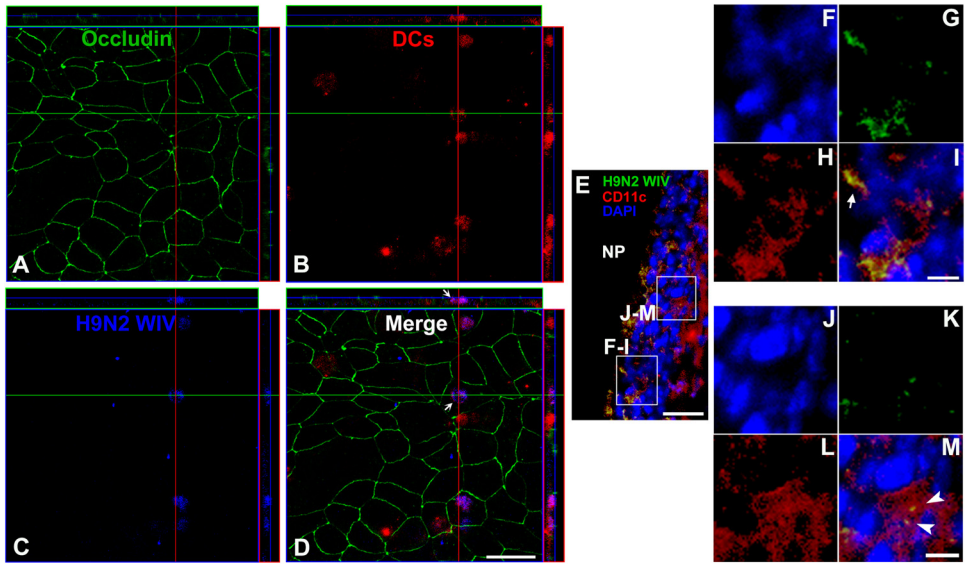

FIG 6 Capture of luminal H9N2 WIV by TEDs after CpG challenge. (A to D) In the *in vitro* coculture system, DyLight 405-labeled H9N2 WIV plus CpGs were incubated on the apical side of the Calu-3 monolayer for 1 h. The filters were processed for CLSM. In views taken between the apical side and the filter, cross-sectional images show that TEDs (dyed with CMTMR, red) were crossing the TJs (occludin, green) of ECs. Internalization of viruses by TEDs was also observed (arrows). The results shown are from a representative experiment out of three. (E to M) The results of the *in vivo* experiment showed capture of H9N2 WIV by DCs in the nasal passage. Mice ($n = 5$) were nasally administered H9N2 WIV plus CpGs for 0.5 h, and then noses were collected. (E) Enlargements of the regions in the white frames are shown in panels F to I or J to M. (F to I) The TEDs sampled the viruses (arrow). (J to M) The virus-loaded DCs (arrowheads) moved away from the ECs. Red (CD11c), DCs; blue (DAPI), nuclei; green, H9N2 WIV. Bars: 10 μm (A to D); 20 μm (E); 5 μm (F to M).

To understand what molecular cues DCs used for uptake of H9N2 WIV, we focused on the DC receptors that could participate in H9N2 WIV capture. SIGN-related 1 (SIGN-R1), a C-type lectin, shares homology with the human DC-specific intercellular adhesion molecule DC-SIGN (35). SIGN-R1 is known to bind carbohydrate structures like dextran (36) and capture pathogens from the blood, including yeast (37) and encapsulated bacteria like *Streptococcus pneumoniae* (38). SIGN-R1 is also an important receptor for the capture of inactivated influenza virus by medullary DCs (39). We hypothesized that nasal DCs might also be equipped with SIGN-R1 to facilitate H9N2 WIV uptake. *In vivo*, we confirmed that SIGN-R1 was highly expressed on lamina propria DCs (Fig. 7A to D) and TEDs (Fig. 7E to H). *In vitro*, we first determined that SIGN-R1 was expressed on the GM-CSF-induced DCs (Fig. 7I). Pretreatment of DCs with mannan (a specific inhibitor for C-type lectin receptors [CLRs] [40]) or SIGN-R1-specific blocking antibody but not with isotype IgM impaired the ability of DCs to take up H9N2 WIV (Fig. 7J to O).

CpGs were captured by both ECs and TEDs. To trace the whereabouts of CpGs at an early stage, Calu-3 monolayers were exposed to fluorescent CpGs plus H9N2 WIV or medium for 1 h (Fig. 8Aa). As shown by the results in Fig. 8B and C, CpGs but not H9N2 WIV were able to get into the ECs, which is a vital step for the interaction between CpGs and intracellular TLR9 (22, 41) or between influenza virus and intracellular TLR7 (42). The interaction between CpGs and submucosal DCs is required for direct activation of DCs (43), so we asked whether TEDs of DCs could capture luminal CpGs. In the DC/EC coculture system (Fig. 8Ab), the *z*-orthogonal view showed that submucosal DCs sent TEDs across tight junctions to sample luminal fluorescence-labeled CpGs (Fig. 8D). We also observed that both CpGs and H9N2 WIV were internalized by the basolateral bodies of DCs (Fig. 8 Ac and E to H).

Chemokine CCL20 and TLR9 signaling pathways were involved in DC recruitment and TED formation in the nasal passage. To better understand the molecular cues required for DC recruitment and TED formation in the nasal passage, we examined the role of chemokine and TLR9 pathways. CCL20 is known to be secreted by intestinal ECs in response to TLR stimuli, and it attracts immature DCs that are equipped with the CCR6 receptor to the epithelium (44, 45). We assessed the expression of CCL20 in the nasal passage mucosa after CpG challenge. Immunofluorescence analysis of cryosections showed that CpGs but not PBS induced CCL20 expression in ECs (Fig. 9A to C and F). Of note, TED formation likely occurred in CCL20-enriched epithelial regions (Fig. 9C, arrowheads). Immunofluorescence analysis revealed that CCL20 was mainly distributed in the apical side of ECs (Fig. 9A to C), which might be highly conducive to DC recruitment and TED formation in the direction of the concentration gradient. As expected, CpGs significantly induced DC recruitment (Fig. 9G) and TED formation (Fig. 9H) in the submucosal regions compared with the results for PBS. However, pretreatment with anti-CCL20 neutralizing antibody but not with the normal IgG control significantly attenuated the number of TEDs in ECs (Fig. 9H). These virus-loaded DCs quickly migrated into the draining CLNs for processing and presenting of antigens. Therefore, we collected the CLN cells after nasal instillation of PBS, CpGs, H9N2 WIV alone, or H9N2 WIV plus CpGs or CT. FACS analyses indicated that CpGs or CT significantly increased the number of H9N2 WIV-loaded DCs in CLNs. Interestingly, pretreatment with CQ or anti-CCL20 neutralizing

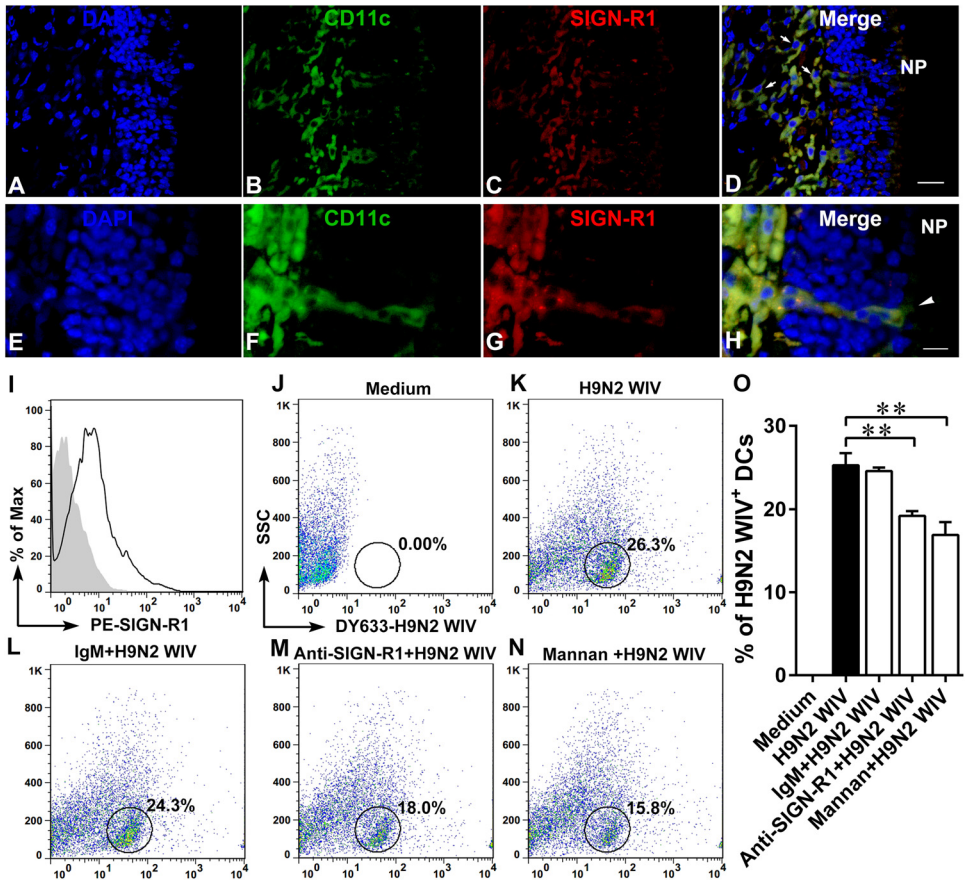

FIG 7 Expression of SIGN-R1 receptor on DCs is conducive to H9N2 WIV uptake. Mice ($n = 5$) were nasally administered H9N2 WIV plus CpGs for 0.5 h, and then noses were collected. (A to H) CLSM analysis of SIGN-R1 receptor located in lamina propria DCs (A to D) or in TEDs (E to H). Blue, DAPI; green, CD11c; red, SIGN-R1; yellow, merge; arrows, lamina propria DCs; arrowheads, TEDs. Bars: 20 μm (A to D); 10 μm (E to H). (I) Histogram showing the results of FACS analysis of SIGN-R1 expression on DCs *in vitro*. Filled gray, isotype control; black line, stained cells. (J to O) *In vitro*, DCs were pretreated with or without SIGN-R1-specific blocking antibody (20 μg/ml) or isotype IgM (20 μg/ml) or mannan (1 mg/ml) for 30 min at 37°C and then incubated with DyLight 633-labeled H9N2 WIV (HA concentration of 10 μg/ml) for 30 min. (J to N) FACS analyses of viral uptake by DCs. SSC, side scatter. (O) Quantification of the FACS results as shown in panels J to N. Data shown are the mean results ± SD from three samples. *, $P < 0.05$; **, $P < 0.01$. The results are representative of three independent experiments.

antibody but not with the normal IgG control significantly attenuated the number of virus-loaded DCs in CLNs, although CpGs were also administered (Fig. 9I and J). These data, combined with the results shown in Fig. 8, revealed that CpGs might first enter into the ECs, activate the TLR9 signaling pathway, strongly stimulate ECs to secrete CCL20, which recruits more DCs into the submucosal regions, and then further induce TED formation for viral uptake, after which the virus-loaded DCs quickly migrate into CLNs for antigen presentation.

DISCUSSION

CpG oligodeoxynucleotides, as a mucosal adjuvant, have been mainly focused on the direct activation of myeloid DCs, plasmacytoid dendritic cells (pDCs), and B cells via TLR9-mediated recognition (22). Here, we describe experiments showing that CpGs also played an important role in facilitating the delivery of H9N2 WIV across the nasal mucosal barriers at an early stage of mucosal immunity. Using a DC/EC coculture system *in vitro* and nasal instillation *in vivo*, we have shown that CpGs, as foreign danger signals, can recruit numerous DCs to the nasal epithelium quickly and prompt them to form TEDs for capturing luminal H9N2 WIV. Meanwhile, CpGs were also captured by TEDs. Subsequently, accompanied by gradual DC maturation, virus-loaded DCs migrated into the draining CLNs for presentation. Under the comprehensive functioning of CpGs and antigens, adaptive immunity was finally initiated.

Inactivated influenza viruses alone were not enough to induce effective nasal mucosal immune responses after intranasal immunization, due to the loss of replication in the epithelium of the respiratory tract. Our current data and previous studies (3) clearly demonstrate that CpGs can strongly facilitate the stimulation by H9N2 WIV to improve the local mucosal and systemic immune responses. As is well known, the crossing of mucosal barriers by antigens is a key step for initiating subsequent antigen-specific immune responses, and not just in activating innate immunity by using various adjuvants. We have shown that H9N2 WIV only attached to the apical surface of the ECs, implying that CpGs could give assistance to the transepithelial transport of H9N2 WIV. Indeed, live influenza viruses, including human H3N2 and avian H5N1 viruses, enter and release principally from the apical side of Calu-3 cells and not the basolateral side (46).

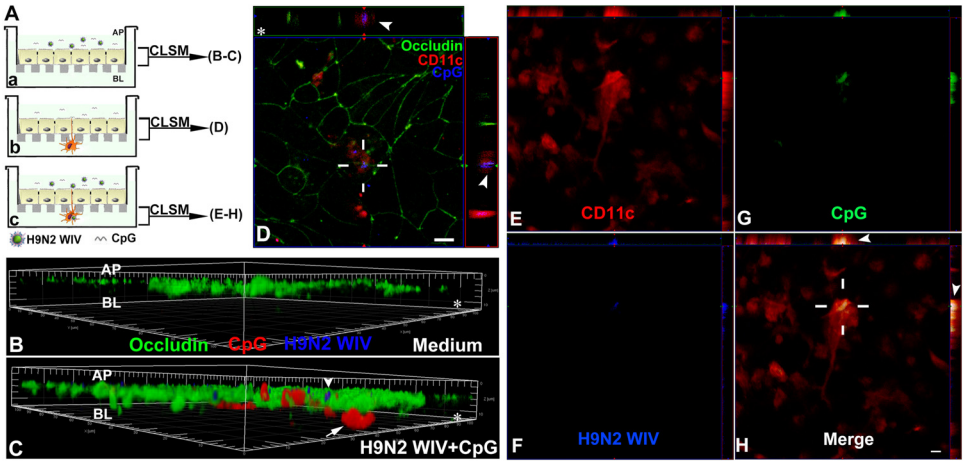

FIG 8 Uptake of CpGs by both ECs and TEDs. (A) Schematic depicting the Calu-3 monolayer, where DyLight 405-labeled H9N2 WIV plus Alexa Fluor 594-CpGs were seeded on the apical side of the ECs for 1 h (a), and the *in vitro* DC/EC coculture system, where Alexa Fluor 594-CpGs alone (b) or plus DyLight 405-labeled H9N2 WIV (c) were incubated on the apical side of the Calu-3 monolayer for 1 h. The filters were processed for CLSM. AP, apical side; BL, basolateral side. (B and C) Three-dimensional rendering of representative images obtained using Imaris 7.2 software. (C) Viruses (blue, arrowhead) were only on the apical side of ECs, whereas CpGs (red, arrow) could enter into the ECs. (D) In views taken between the apical side and the filter, cross-sectional images show that TEDs (red [CD11c], arrowheads) crossed the TJs of ECs (occludin, green) and captured the CpGs (blue). (E to H) In views taken between the filter and the basolateral side, cross-sectional images show that both H9N2 WIV (blue) and CpGs (green) existed within submucosal DCs (red [CD11c], arrowheads). The results shown are from a representative experiment out of three. Asterisks indicate the filter. (D to H) Bars: 10 μm.

We further found that the number of virus-loaded submucosal DCs was increased in response to H9N2 WIV plus CpGs in an *in vitro* DC/Calu-3 polarized culture, supporting the idea that CpGs assisted H9N2 WIV in transepithelial delivery.

Transcytosis and paracellular transport are the main epithelial transport pathways (47). To understand whether ECs participate in viral transepithelial delivery after CpG treatment, we established an indirect system to assess the EC functions. Interestingly, in this system, it was difficult to find any viruses within the DCs or the ECs, and furthermore, the indexes of paracellular transport, including TEER and tight junctions, were not altered, indicating that submucosal DCs but not ECs played a dominant role in viral transport in the coculture system. Consistent with a recent report (48), the typical mucosal adjuvant CT, in contrast to CpGs, strongly disrupted the EC barrier function, implying another adjuvant mechanism whereby CT can facilitate antigen transport via the epithelial paracellular pathway.

Another possibility for the increase of viral transepithelial transport in the presence of CpGs is mediated by the TEDs of submucosal DCs. TLRs are PRRs that recognize structurally conserved molecules derived from microbes (49). In the small bowel, TLR signaling by epithelial elements plays a key role in the DC extension response (50). In the DC/Caco-2 intestinal EC coculture system, LPS induced DCs to form dendrites across the EC layer (18). Nasal epithelial cells also express various TLRs, including TLR9 (51), implying that TED formation might facilitate effective antigen uptake in the upper respiratory tract. However, controversially, in the nasal passage, TEDs were observed in allergic rhinitis (19) but not in response to luminal pathogens, such as group A *Streptococcus* (GAS) (52). In the lung, TEDs were easily formed in the alveolar DCs but not in airway DCs (53). Here, our *in vivo* data and the data from our *in vitro* coculture system provided strong evidence that, after CpG administration, nasal airway DCs can form TEDs to sample luminal H9N2 WIV.

The surface epithelium lining the nasal passages is often the first tissue to be directly stimulated by foreign danger signals. It is mainly composed of stratified squamous epithelium, simple cuboidal epithelium, and pseudostratified columnar ciliated epithelium (54). A previous study discovered a route by which some pathogenic microorganisms can invade through ECs via intraepithelial DCs, because the DCs between the intestinal epithelial cells are reported to express tight junction proteins, such as occludin, claudin 1, and ZO-1 (17). In the nasal epithelium, continuous tight junction strands formed well-developed barriers (19). We also provide evidence that DCs sent out their TEDs across tight junctions of the nasal epithelium for viral capture, especially after the addition of CpGs. Interestingly, the TEDs were easily found in the nasal passage but not in NALT, though virus-loaded DCs were also found after 1.5 h (data not shown), suggesting that CpGs always preferred to mobilize submucosal DCs in the nasal passage. The presence of M cells in NALT, a key participant in the antigen uptake, might imply that TEDs are not necessary in this zone. Recently, in the intestinal Peyer's patch, an organized lymphoid nodule similar to NALT, it was found that only one specific subtype of DCs (LysoDCs) sent their dendrites through M cell-specific transcellular pores but not classic paracellular processes (55), implying that TED formation is not in fact universal in Peyer's patches.

There is an ongoing controversy over which members of the DC subpopulations participate in TED formation in the small intestine. Previously, $CX3CR1^+$ DCs rather than $CD103^+$ DCs have been consistently observed to sample the intestinal luminal content by extending TEDs (56–58). Recently, $CD103^+$ DCs have been shown to be capable of efficiently sampling luminal bacteria by using their intraepithelial dendrites and then migrating into the mesenteric lymph nodes (57, 59). In the lung, $CD103^+$ DCs have been shown to play important roles in response to viruses (including influenza virus) (60), allergens (53), and apoptotic cells (61) and then to traffic them to the draining lymph node for presenta-

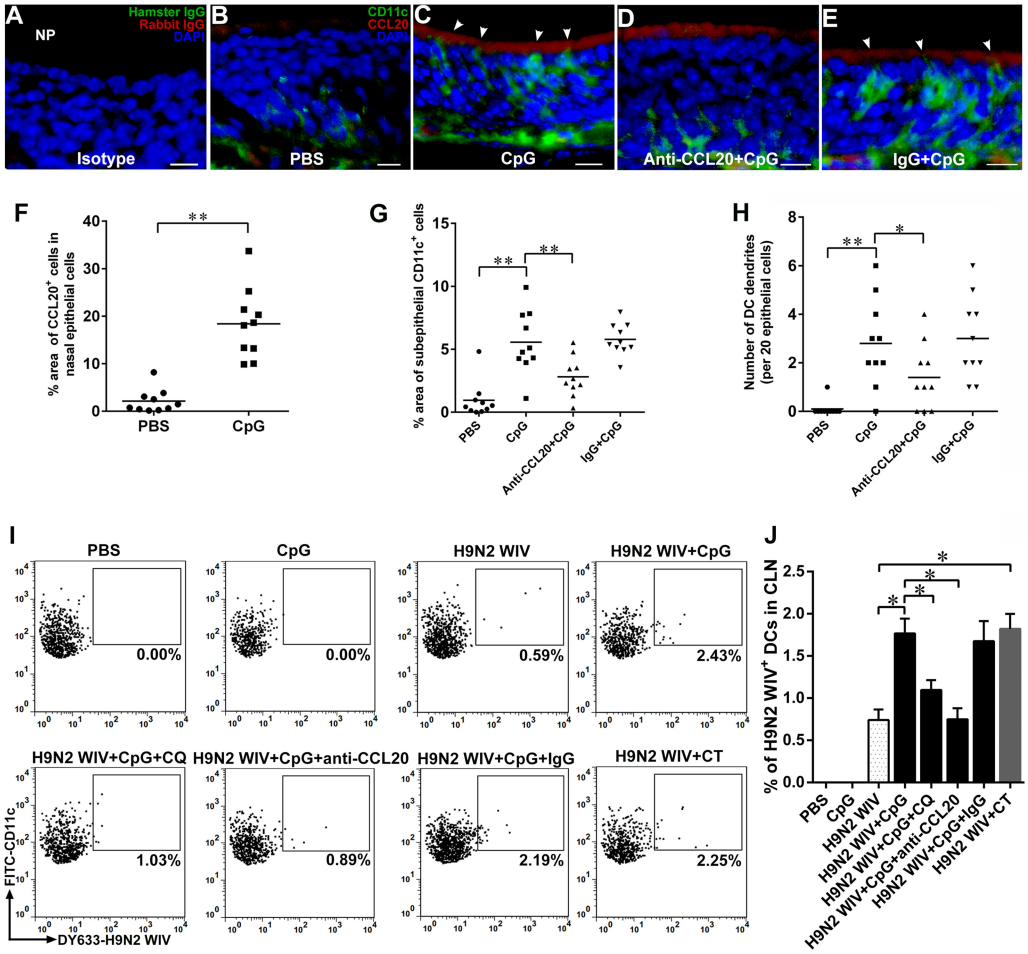

FIG 9 The role of CCL20 in DC recruitment and TED formation in nasal passage after CpG challenge. (A to H) CCL20 neutralizing antibody (100 μg) or rabbit IgG control was administered to mice ($n = 6$) intraperitoneally for 2 h, and then PBS or CpGs (20 μg) were intranasally instilled in mice for 0.5 h, and noses were collected. (A to E) Immunofluorescence staining of nasal passage. Frozen sections were stained with CD11c (green), DAPI (blue), and CCL20 (red). (A) Isotype control. Bars: 10 μm. (F and G) Quantification of the cells positive for CCL20 (F) or CD11c (G) in the nasal passage is displayed in scatter plots. The results are expressed as the percentage of the area occupied by positive cells compared to that of ECs (F) or lamina propria (G). (H) The number of TEDs was quantified. Values are expressed as the number of TEDs per 20 ECs. Each dot represents the value obtained from 1 field of 10 random fields from 6 mice. Horizontal lines across the scatter plots represent mean values. (I) Chloroquine (CQ; 10 mg/kg of body weight), CCL20 neutralizing antibody (100 μg), or rabbit IgG control was administered to mice ($n = 6$) intraperitoneally for 2 h, and then PBS, CpGs (20 μg), or DyLight 633-labeled H9N2 WIV (20 μg HA) alone or plus CpGs (20 μg) or CT (2 μg) was intranasally instilled in the mice for 2 h. CLN cells were isolated and analyzed by FACS. (J) Quantification of the FACS results as shown in panel I. The data shown are the mean results ± SD from three samples. *, $P < 0.05$; **, $P < 0.01$.

tion (62). $CD103^+$ DCs also express the tight junction proteins claudin 1, claudin 7, and zonula occludens 2, which could form tight junctions with airway epithelial cells (63), as in the gut (17). However, there is no direct evidence that $CD103^+$ DCs in the lung or upper respiratory tract have the capability of sampling luminal antigens through their TEDs. Here, in experiments in the nasal passage, a site that is distinguishable from the lung, $CD103^+$ DCs participated in the formation of TEDs. Furthermore, although TED formation has been found in the alveolar DCs, it is largely independent of allergen or TLR challenge (53). This differs from the results of a study of dendritic cell extension into the small bowel lumen in response to epithelial cell TLR engagement (50). In our study, similar to the study of the gut, CpGs played a dominant role in facilitating the uptake of H9N2 WIV by TEDs in the nasal passage. One interpretation of these different findings is that, compared to the lung epithelium, the epithelium of the upper respiratory tract, especially that of the nasal passage, always has to face the most complex and dangerous foreign pathogens, resulting in triggering advance warnings and active defenses of the immune system, such as TED formation in nasal submucosal DCs. In these danger zones, some PRRs, such as the TLRs, have rich expressions in ECs. These ideas are also supported by a previous study showing that tracheal DCs were augmented in the subepithelial regions by epithelial TLR4 stimulation (64). In fact, TLR4 expression is vastly different between the trachea and the lung (53).Thus, it is likely that regional disparities in the epithelium play an important role in determining responses to inhaled vaccines at different sites.

Inactivated influenza viruses are perceived by the nasal ECs as much less dangerous than live viruses. Previously, lamina propria DCs were found to form TEDs in response to TLR stimuli (LPS or other bacterial products) in the DC/Caco-2

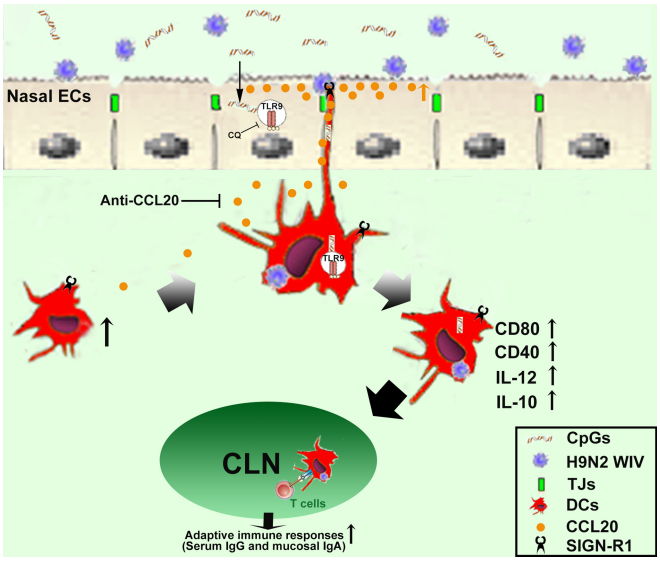

FIG 10 Schematic of proposed mechanism for CpG-induced enhancement of the transepithelial transport of H9N2 WIV in nasal mucosa. CpGs first entered into the ECs, activated the TLR9 signaling pathway, and strongly stimulated ECs to secrete CCL20, which recruited more DCs into the submucosal regions. The polarity distribution of CCL20 provided the possibility for TED formation. The presence of SIGN-R1 receptor on TEDs provided more possibilities for viral capture. After capture of the viruses and CpGs by TEDs, DCs gradually matured (phenotypic and functional maturation) and then quickly migrated into draining CLNs for antigen presentation. Finally, the antigen-specific immune response was initiated.

intestinal EC coculture system *in vitro* (18) and an intestinal ligated-loop model *in vivo* (50), implying that TLR stimuli could be a potential helper in antigen delivery. Our data suggest that CpGs, as typical TLR agonists, not only enhanced the downstream H9N2 WIV-specific immune responses but also, as danger signals, strongly improved the sensitivity of ECs via activating TLR9 signaling pathway in response to antigens. The ECs quickly released the chemokine CCL20 and mobilized DCs to accumulate in the submucosal regions. The polarity distribution of CCL20 could provide the possibility for TED formation. More subtle concentration gradients may occur, as CCL20 is released by nasal ECs into lateral intercellular spaces before diffusing into the connective tissue below. The recruited DCs, using remarkable shape-shifting abilities, make their part of the body migrate into the ECs. The typical lines of supporting evidence were from the stratified epithelia of tonsils, skin, and vagina during inflammation. Complementary chemokine gradients were found within the epithelium itself, and CCL20 expression in the most apical cell layers accounts for DC migration of Langerhans cell precursors into the epithelium (65, 66). For the single-layered epithelium of the intestine, the results from our (data not shown) and other studies (67) also support the above-described views.

Conclusions. Our results suggest a new mechanism by which CpGs assist the H9N2 WIV in crossing the nasal epithelial barriers via transepithelial uptake of TEDs (Fig. 10). A novel strategy would be to develop improved antigen delivery through mobilizing broad submucosal DCs to capture luminal antigens using their TEDs.

ACKNOWLEDGMENTS

This work was supported by the National Natural Science Foundation of China (grant 31172302) and Priority Academic Program Development (PAPD) of Jiangsu Higher Education Institutions.

All authors declare that they have no competing interests.

REFERENCES

1. **Gao R, Cao B, Hu Y, Feng Z, Wang D, Hu W, Chen J, Jie Z, Qiu H, Xu K, Xu X, Lu H, Zhu W, Gao Z, Xiang N, Shen Y, He Z, Gu Y, Zhang Z, Yang Y, Zhao X, Zhou L, Li X, Zou S, Zhang Y, Yang L, Guo J, Dong J, Li Q, Dong L, Zhu Y, Bai T, Wang S, Hao P, Yang W, Han J, Yu H, Li D, Gao GF, Wu G, Wang Y, Yuan Z, Shu Y.** 2013. Human infection with a novel avian-origin influenza A (H7N9) virus. N Engl J Med **368:** 1888–1897. http://dx.doi.org/10.1056/NEJMoa1304459.
2. **Xiong X, Martin SR, Haire LF, Wharton SA, Daniels RS, Bennett MS, McCauley JW, Collins PJ, Walker PA, Skehel JJ, Gamblin SJ.** 2013. Receptor binding by an H7N9 influenza virus from humans. Nature **499:** 496–499. http://dx.doi.org/10.1038/nature12372.
3. **Kang H, Wang H, Yu Q, Yang Q.** 2012. Effect of intranasal immunization with inactivated avian influenza virus on local and systemic immune responses in ducks. Poult Sci **91:**1074–1080. http://dx.doi.org/10.3382/ps.2011-01817.
4. **Rose MA, Zielen S, Baumann U.** 2012. Mucosal immunity and nasal influenza vaccination. Expert Rev Vaccines **11:**595–607. http://dx.doi.org/10.1586/erv.12.31.
5. **Chen H.** 2009. Avian influenza vaccination: the experience in China. Rev Sci Tech **28:**267–274.
6. **Geeraedts F, Goutagny N, Hornung V, Severa M, de Haan A, Pool J, Wilschut J, Fitzgerald KA, Huckriede A.** 2008. Superior immunogenicity of inactivated whole virus H5N1 influenza vaccine is primarily controlled by Toll-like receptor signalling. PLoS Pathog **4:**e1000138. http://dx.doi.org/10.1371/journal.ppat.1000138.
7. **Illum L.** 2003. Nasal drug delivery—possibilities, problems and solutions. J Control Release **87:**187–198. http://dx.doi.org/10.1016/S0168-3659(02)00363-2.
8. **Wu Y, Wei W, Zhou M, Wang Y, Wu J, Ma G, Su Z.** 2012. Thermal-sensitive hydrogel as adjuvant-free vaccine delivery system for H5N1 intranasal immunization. Biomaterials **33:**2351–2360. http://dx.doi.org/10.1016/j.biomaterials.2011.11.068.
9. **Tamura S, Samegai Y, Kurata H, Nagamine T, Aizawa C, Kurata T.** 1988. Protection against influenza virus infection by vaccine inoculated intranasally with cholera toxin B subunit. Vaccine **6:**409–413. http://dx.doi.org/10.1016/0264-410X(88)90140-5.
10. **Couch RB, Atmar RL, Cate TR, Quarles JM, Keitel WA, Arden NH, Wells J, Nino D, Wyde PR.** 2009. Contrasting effects of type I interferon as a mucosal adjuvant for influenza vaccine in mice and humans. Vaccine **27:**5344–5348. http://dx.doi.org/10.1016/j.vaccine.2009.06.084.
11. **Yang P, Tang C, Luo D, Zhan Z, Xing L, Duan Y, Jia W, Peng D, Liu X, Wang X.** 2010. Cross-clade protection against HPAI H5N1 influenza virus challenge in BALB/c mice intranasally administered adjuvant-combined influenza vaccine. Vet Microbiol **146:**17–23. http://dx.doi.org/10.1016/j.vetmic.2010.03.024.
12. **Fu J, Liang J, Kang H, Lin J, Yu Q, Yang Q.** 2013. Effects of different CpG oligodeoxynucleotides with inactivated avian H5N1 influenza virus on mucosal immunity of chickens. Poult Sci **92:**2866–2875. http://dx.doi.org/10.3382/ps.2013-03205.
13. **Zhang XW, Yu QH, Zhang XF, Yang Q.** 2009. Co-administration of inactivated avian influenza virus with CpG or rIL-2 strongly enhances the local immune response after intranasal immunization in chicken. Vaccine **27:**5628–5632. http://dx.doi.org/10.1016/j.vaccine.2009.07.023.
14. **Xiang XX, Zhou XQ, Xie Q, Yu H, Zhou HJ.** 2008. Effects of CpG-ODN combined with HBsAg on the phenotype, function and the activity of NF-kappa B and AP-1 of monocyte-derived dendritic cells in chronic hepatitis B patients. Zhonghua Gan Zang Bing Za Zhi **16:**97–100. (In Chinese.)
15. **Lambrecht BN, Hammad H.** 2003. Taking our breath away: dendritic cells in the pathogenesis of asthma. Nat Rev Immunol **3:**994–1003. http://dx.doi.org/10.1038/nri1249.
16. **Kiyono H, Fukuyama S.** 2004. NALT- versus Peyer's-patch-mediated mucosal immunity. Nat Rev Immunol **4:**699–710. http://dx.doi.org/10.1038/nri1439.
17. **Rescigno M, Urbano M, Valzasina B, Francolini M, Rotta G, Bonasio R,**

Granucci F, Kraehenbuhl JP, Ricciardi-Castagnoli P. 2001. Dendritic cells express tight junction proteins and penetrate gut epithelial monolayers to sample bacteria. Nat Immunol **2:**361–367. http://dx.doi.org/10.1038/86373.

18. **Rimoldi M, Chieppa M, Vulcano M, Allavena P, Rescigno M.** 2004. Intestinal epithelial cells control dendritic cell function. Ann NY Acad Sci **1029:**66–74. http://dx.doi.org/10.1196/annals.1309.009.
19. **Takano K, Kojima T, Go M, Murata M, Ichimiya S, Himi T, Sawada N.** 2005. HLA-DR- and CD11c-positive dendritic cells penetrate beyond well-developed epithelial tight junctions in human nasal mucosa of allergic rhinitis. J Histochem Cytochem **53:**611–619. http://dx.doi.org/10.1369/jhc.4A6539.2005.
20. **Niess JH, Brand S, Gu X, Landsman L, Jung S, McCormick BA, Vyas JM, Boes M, Ploegh HL, Fox JG, Littman DR, Reinecker HC.** 2005. CX3CR1-mediated dendritic cell access to the intestinal lumen and bacterial clearance. Science **307:**254–258. http://dx.doi.org/10.1126/science.1102901.
21. **Cardon LR, Burge C, Clayton DA, Karlin S.** 1994. Pervasive CpG suppression in animal mitochondrial genomes. Proc Natl Acad Sci U S A **91:**3799–3803. http://dx.doi.org/10.1073/pnas.91.9.3799.
22. **Klinman DM.** 2004. Immunotherapeutic uses of CpG oligodeoxynucleotides. Nat Rev Immunol **4:**249–258. http://dx.doi.org/10.1038/nri1329.
23. **Witschi C, Mrsny RJ.** 1999. In vitro evaluation of microparticles and polymer gels for use as nasal platforms for protein delivery. Pharm Res **16:**382–390. http://dx.doi.org/10.1023/A:1018869601502.
24. **Amidi M, Romeijn SG, Borchard G, Junginger HE, Hennink WE, Jiskoot W.** 2006. Preparation and characterization of protein-loaded N-trimethyl chitosan nanoparticles as nasal delivery system. J Control Release **111:**107–116. http://dx.doi.org/10.1016/j.jconrel.2005.11.014.
25. **Hartshorn KL, Crouch EC, White MR, Eggleton P, Tauber AI, Chang D, Sastry K.** 1994. Evidence for a protective role of pulmonary surfactant protein D (Sp-D) against influenza A viruses. J Clin Invest **94:**311–319. http://dx.doi.org/10.1172/JCI117323.
26. **Kang H, Yan M, Yu Q, Yang Q.** 2013. Characteristics of nasal-associated lymphoid tissue (NALT) and nasal absorption capacity in chicken. PLoS One **8:**e84097. http://dx.doi.org/10.1371/journal.pone.0084097.
27. **Wang Z, Gao J, Yu Q, Yang Q.** 2012. Oral immunization with recombinant Lactococcus lactis expressing the hemagglutinin of the avian influenza virus induces mucosal and systemic immune responses. Future Microbiol **7:**1003–1010. http://dx.doi.org/10.2217/fmb.12.69.
28. **Wegmann F, Gartlan KH, Harandi AM, Brinckmann SA, Coccia M, Hillson WR, Kok WL, Cole S, Ho LP, Lambe T, Puthia M, Svanborg C, Scherer EM, Krashias G, Williams A, Blattman JN, Greenberg PD, Flavell RA, Moghaddam AE, Sheppard NC, Sattentau QJ.** 2012. Polyethyleneimine is a potent mucosal adjuvant for viral glycoprotein antigens. Nat Biotechnol **30:**883–888. http://dx.doi.org/10.1038/nbt.2344.
29. **Barnier-Quer C, Elsharkawy A, Romeijn S, Kros A, Jiskoot W.** 2013. Adjuvant effect of cationic liposomes for subunit influenza vaccine: influence of antigen loading method, cholesterol and immune modulators. Pharmaceutics **5:**392–410. http://dx.doi.org/10.3390/pharmaceutics5030392.
30. **Yin Y, Qin T, Yu Q, Yang Q.** 2014. Bursopentin (BP5) from chicken bursa of fabricius attenuates the immune function of dendritic cells. Amino Acids **46:**1763–1774. http://dx.doi.org/10.1007/s00726-014-1735-x.
31. **Foster KA, Avery ML, Yazdanian M, Audus KL.** 2000. Characterization of the Calu-3 cell line as a tool to screen pulmonary drug delivery. Int J Pharm **208:**1–11. http://dx.doi.org/10.1016/S0378-5173(00)00452-X.
32. **Sakuraba A, Sato T, Kamada N, Kitazume M, Sugita A, Hibi T.** 2009. Th1/Th17 immune response is induced by mesenteric lymph node dendritic cells in Crohn's disease. Gastroenterology **137:**1736–1745. http://dx.doi.org/10.1053/j.gastro.2009.07.049.
33. **Guermonprez P, Valladeau J, Zitvogel L, Thery C, Amigorena S.** 2002. Antigen presentation and T cell stimulation by dendritic cells. Annu Rev Immunol **20:**621–667. http://dx.doi.org/10.1146/annurev.immunol.20.100301.064828.
34. **Itagaki K, Adibnia Y, Sun SQ, Zhao C, Sursal T, Chen Y, Junger W, Hauser CJ.** 2011. Bacterial DNA induces pulmonary damage via TLR-9 through cross-talk with neutrophils. Shock **36:**548–552. http://dx.doi.org/10.1097/SHK.0b013e3182369fb2.
35. **Geijtenbeek TBH, Groot PC, Nolte MA, van Vliet SJ, Gangaram-Panday ST, van Duijnhoven GCF, Kraal G, van Oosterhout AJM, van Kooyk Y.** 2002. Marginal zone macrophages express a murine homologue of DC-SIGN that captures blood-borne antigens in vivo. Blood **100:**2908–2916. http://dx.doi.org/10.1182/blood-2002-04-1044.
36. **Kang YS, Yamazaki S, Iyoda T, Pack M, Bruening SA, Kim JY, Takahara K, Inaba K, Steinman RM, Park CG.** 2003. SIGN-R1, a novel C-type lectin expressed by marginal zone macrophages in spleen, mediates uptake of the polysaccharide dextran. Int Immunol **15:**177–186. http://dx.doi.org/10.1093/intimm/dxg019.
37. **Taylor PR, Brown GD, Herre J, Williams DL, Willment JA, Gordon S.** 2004. The role of SIGNR1 and the beta-glucan receptor (Dectin-1) in the nonopsonic recognition of yeast by specific macrophages. J Immunol **172:**1157–1162. http://dx.doi.org/10.4049/jimmunol.172.2.1157.
38. **Kang YS, Kim JY, Bruening SA, Pack M, Charalambous A, Pritsker A, Moran TM, Loeffler JM, Steinman RM, Park CG.** 2004. The C-type lectin SIGN-R1 mediates uptake of the capsular polysaccharide of Streptococcus pneumoniae in the marginal zone of mouse spleen. Proc Natl Acad Sci U S A **101:**215–220. http://dx.doi.org/10.1073/pnas.0307124101.
39. **Gonzalez SF, Lukacs-Kornek V, Kuligowski MP, Pitcher LA, Degn SE, Kim YA, Cloninger MJ, Martinez-Pomares L, Gordon S, Turley SJ, Carroll MC.** 2010. Capture of influenza by medullary dendritic cells via SIGN-R1 is essential for humoral immunity in draining lymph nodes. Nat Immunol **11:**427–434. http://dx.doi.org/10.1038/ni.1856.
40. **Zietara N, Lyszkiewicz M, Puchalka J, Pei G, Gutierrez MG, Lienenklaus S, Hobeika E, Reth M, Martins dos Santos VAP, Krueger A, Weiss S.** 2013. Immunoglobulins drive terminal maturation of splenic dendritic cells. Proc Natl Acad Sci U S A **110:**2282–2287. http://dx.doi.org/10.1073/pnas.1210654110.
41. **McGettrick AF, O'Neill LAJ.** 2010. Localisation and trafficking of Toll-like receptors: an important mode of regulation. Curr Opin Immunol **22:**20–27. http://dx.doi.org/10.1016/j.coi.2009.12.002.
42. **Diebold SS, Kaisho T, Hemmi H, Akira S, Reis e Sousa C.** 2004. Innate antiviral responses by means of TLR7-mediated recognition of single-stranded RNA. Science **303:**1529–1531. http://dx.doi.org/10.1126/science.1093616.
43. **Mutwiri GK, Nichani AK, Babiuk S, Babiuk LA.** 2004. Strategies for enhancing the immunostimulatory effects of CpG oligodeoxynucleotides. J Control Release **97:**1–17. http://dx.doi.org/10.1016/j.jconrel.2004.02.022.
44. **Izadpanah A, Dwinell MB, Eckmann L, Varki NM, Kagnoff MF.** 2001. Regulated MIP-3alpha/CCL20 production by human intestinal epithelium: mechanism for modulating mucosal immunity. Am J Physiol Gastrointest Liver Physiol **280:**G710–G719.
45. **Sierro F, Dubois B, Coste A, Kaiserlian D, Kraehenbuhl JP, Sirard JC.** 2001. Flagellin stimulation of intestinal epithelial cells triggers CCL20-mediated migration of dendritic cells. Proc Natl Acad Sci U S A **98:**13722–13727. http://dx.doi.org/10.1073/pnas.241308598.
46. **Zeng H, Goldsmith C, Thawatsupha P, Chittaganpitch M, Waicharoen S, Zaki S, Tumpey TM, Katz JM.** 2007. Highly pathogenic avian influenza H5N1 viruses elicit an attenuated type I interferon response in polarized human bronchial epithelial cells. J Virol **81:**12439–12449. http://dx.doi.org/10.1128/JVI.01134-07.
47. **Nielsen HM.** 2014. Epithelial permeation and absorption mechanisms of biopharmaceuticals, p 99–122. *In* das Neves J, Sarmento G (ed), Mucosal delivery of biopharmaceuticals. Springer, New York, NY.
48. **Guichard A, Cruz-Moreno B, Aguilar B, van Sorge NM, Kuang J, Kurkciyan AA, Wang Z, Hang S, Pineton de Chambrun GP, McCole DF, Watnick P, Nizet V, Bier E.** 2013. Cholera toxin disrupts barrier function by inhibiting exocyst-mediated trafficking of host proteins to intestinal cell junctions. Cell Host Microbe **14:**294–305. http://dx.doi.org/10.1016/j.chom.2013.08.001.
49. **Akira S.** 2006. TLR signaling. Curr Top Microbiol Immunol **311:**1–16.
50. **Chieppa M, Rescigno M, Huang AYC, Germain RN.** 2006. Dynamic imaging of dendritic cell extension into the small bowel lumen in response to epithelial cell TLR engagement. J Exp Med **203:**2841–2852. http://dx.doi.org/10.1084/jem.20061884.
51. **Tengroth L, Millrud CR, Kvarnhammar AM, Kumlien Georen S, Latif L, Cardell LO.** 2014. Functional effects of Toll-like receptor (TLR)3, 7, 9, RIG-I and MDA-5 stimulation in nasal epithelial cells. PLoS One **9:**e98239. http://dx.doi.org/10.1371/journal.pone.0098239.
52. **Kim DY, Sato A, Fukuyama S, Sagara H, Nagatake T, Kong IG, Goda K, Nochi T, Kunisawa J, Sato S, Yokota Y, Lee CH, Kiyono H.** 2011. The airway antigen sampling system: respiratory M cells as an alternative gateway for inhaled antigens. J Immunol **186:**4253–4262. http://dx.doi.org/10.4049/jimmunol.0903794.
53. **Thornton EE, Looney MR, Bose O, Sen D, Sheppard D, Locksley R, Huang X, Krummel MF.** 2012. Spatiotemporally separated antigen up-

take by alveolar dendritic cells and airway presentation to T cells in the lung. J Exp Med **209:**1183–1199. http://dx.doi.org/10.1084/jem.20112667.
54. **Harkema JR, Carey SA, Wagner JG.** 2006. The nose revisited: A brief review of the comparative structure, function, and toxicologic pathology of the nasal epithelium. Toxicol Pathol **34:**252–269. http://dx.doi.org/10.1080/01926230600713475.
55. **Lelouard H, Fallet M, de Bovis B, Meresse S, Gorvel JP.** 2012. Peyer's patch dendritic cells sample antigens by extending dendrites through M cell-specific transcellular pores. Gastroenterology **142:**592–601.e3. http://dx.doi.org/10.1053/j.gastro.2011.11.039.
56. **Swiatczak B, Rescigno M.** 2012. How the interplay between antigen presenting cells and microbiota tunes host immune responses in the gut. Semin Immunol **24:**43–49. http://dx.doi.org/10.1016/j.smim.2011.11.004.
57. **Lantier L, Lacroix-Lamande S, Potiron L, Metton C, Drouet F, Guesdon W, Gnahoui-David A, Le Vern Y, Deriaud E, Fenis A, Rabot S, Descamps A, Werts C, Laurent F.** 2013. Intestinal CD103+ dendritic cells are key players in the innate immune control of Cryptosporidium parvum infection in neonatal mice. PLoS Pathog **9:**e1003801. http://dx.doi.org/10.1371/journal.ppat.1003801.
58. **Mazzini E, Massimiliano L, Penna G, Rescigno M.** 2014. Oral tolerance can be established via gap junction transfer of fed antigens from CX3CR1(+) macrophages to CD103(+) dendritic cells. Immunity **40:**248–261. http://dx.doi.org/10.1016/j.immuni.2013.12.012.
59. **Schulz O, Jaensson E, Persson EK, Liu XS, Worbs T, Agace WW, Pabst O.** 2009. Intestinal CD103(+), but not CX3CR1(+), antigen sampling cells migrate in lymph and serve classical dendritic cell functions. J Exp Med **206:**3101–3114. http://dx.doi.org/10.1084/jem.20091925.
60. **Hagenaars N, Mania M, de Jong P, Que I, Nieuwland R, Slutter B, Glansbeek H, Heldens J, van den Bosch H, Lowik C, Kaijzel E, Mastrobattista E, Jiskoot W.** 2010. Role of trimethylated chitosan (TMC) in nasal residence time, local distribution and toxicity of an intranasal influenza vaccine. J Control Release **144:**17–24. http://dx.doi.org/10.1016/j.jconrel.2010.01.027.
61. **Desch AN, Randolph GJ, Murphy K, Gautier EL, Kedl RM, Lahoud MH, Caminschi I, Shortman K, Henson PM, Jakubzick CV.** 2011. CD103+ pulmonary dendritic cells preferentially acquire and present apoptotic cell-associated antigen. J Exp Med **208:**1789–1797. http://dx.doi.org/10.1084/jem.20110538.
62. **Lukens MV, Kruijsen D, Coenjaerts FE, Kimpen JL, van Bleek GM.** 2009. Respiratory syncytial virus-induced activation and migration of respiratory dendritic cells and subsequent antigen presentation in the lung-draining lymph node. J Virol **83:**7235–7243. http://dx.doi.org/10.1128/JVI.00452-09.
63. **Sung SSJ, Fu SM, Rose CE, Gaskin F, Ju ST, Beaty SR.** 2006. A major lung CD103 (alphaE)-beta7 integrin-positive epithelial dendritic cell population expressing Langerin and tight junction proteins. J Immunol **176:**2161–2172. http://dx.doi.org/10.4049/jimmunol.176.4.2161.
64. **Hammad H, Chieppa M, Perros F, Willart MA, Germain RN, Lambrecht BN.** 2009. House dust mite allergen induces asthma via Toll-like receptor 4 triggering of airway structural cells. Nat Med **15:**410–416. http://dx.doi.org/10.1038/nm.1946.
65. **Cremel M, Berlier W, Hamzeh H, Cognasse F, Lawrence P, Genin C, Bernengo JC, Lambert C, Dieu-Nosjean MC, Delezay O.** 2005. Characterization of CCL20 secretion by human epithelial vaginal cells: involvement in Langerhans cell precursor attraction. J Leukoc Biol **78:**158–166. http://dx.doi.org/10.1189/jlb.0305147.
66. **Vanbervliet A, Homey B, Durand I, Massacrier C, Ait-Yahia S, de Bouteiller O, Vicari A, Caux C.** 2002. Sequential involvement of CCR2 and CCR6 ligands for immature dendritic cell recruitment: possible role at inflamed epithelial surfaces. Eur J Immunol **32:**231–242. http://dx.doi.org/10.1002/1521-4141(200201)32:1<231::AID-IMMU231>3.0.CO;2-8.
67. **Anosova NG, Chabot S, Shreedhar V, Borawski JA, Dickinson BL, Neutra MR.** 2008. Cholera toxin, E coli heat-labile toxin, and non-toxic derivatives induce dendritic cell migration into the follicle-associated epithelium of Peyer's patches. Mucosal Immunol **1:**59–67. http://dx.doi.org/10.1038/mi.2007.7.